Available online at www.sciencedirect.com

jmr&t Journal of Materials Research and Technology

www.jmrt.com.br

# Poly-thiourea formaldehyde based anticorrosion marine coatings on type 304 stainless steel

*Sehrish Kanwal*[a], *Naveed Zafar Ali*[b,c], *Rizwan Hussain*[c], *Faiz Ullah Shah*[d], *Zareen Akhter*[a,*]

[a] *Department of Chemistry, Quaid-i-Azam University, Islamabad, Pakistan*
[b] *Federal Institute for Materials Research and Testing (BAM), Richard-Willstaetter-Strasse 11, Berlin 12489, Germany*
[c] *Laboratory for Advanced Materials & Processing (LAMP) National Centre for Physics, Quaid-i-Azam University Campus, Islamabad, Pakistan*
[d] *Chemistry of Interfaces, Luleå University of Technology, 971 87 Luleå, Sweden*

ARTICLE INFO

*Article history:*
Received 10 July 2019
Accepted 14 December 2019
Available online 6 January 2020

*Keywords:*
In-situ polymerization
Encapsulation
Thiourea-formaldehyde
Marine corrosion

ABSTRACT

In the present study, hexamethylene diisocyanate (HMDI) encapsulated poly-thiourea formaldehyde (PTF) (10 wt%) coating was developed in an epoxy-polyamine matrix and their anticorrosion studies on Type SS304 stainless steel substrate have been conducted using electrochemistry techniques. The compact and hydrophobic shell wall of PTF proved to be a potent shell wall material for HMDI encapsulation. The effect of temperature and pH values was found to be decisive factor in the synthesis of microcapsules. The PTF microcapsules were synthesized in acidic condition with a pH value of 3. Over 90% of the core fraction is retained in water after 21 days immersion. However, core content decreased with increasing temperature. The capsules were characterized by Fourier transform infrared spectroscopy (FTIR), scanning electron microscopy (SEM), thermogravimetric analysis (TGA) and Electrochemical Impedance spectroscopy (EIS). Scanning electron microscopic analysis depicts the uniform morphology of coating with a particle size in the range of 1.08 μm–22.06 μm. The vibrational band at 2271 $cm^{-1}$ attributed to NCO signal further endorses the successful encapsulation of HMDI into the PTF capsules. Electrochemical testing on steel specifies the appreciable anticorrosion performance of the synthesized poly thiourea formaldehyde (PTF) coating against artificial sea water.



## 1. Introduction

The total cost of corrosion globally amounts to ~2.5 trillion US dollars per year. Various strategies conventionally employed to protect metal from corrosion include cathodic protection [1,2] corrosion inhibitors [3–7] conversion [8,9] and organic coatings [10–12]. Among these, organic protective coatings are the most widely used material in corrosion mitigation measure [7]. Microencapsulation technology is introduced in recent years to develop smart materials for corrosion prevention. The microcapsule incorporating core material is dispersed into a polymer-based matrix to form a composite. Capsules loaded with functional core materials have been used in various fields such as ecology, drug release [13], textiles [14], cosmetics [15], printing [16], fire resistance powders [17,18],

* Corresponding author.
E-mails: naveednik@gmail.com (N.Z. Ali), zareenakhter@yahoo.com (Z. Akhter).
https://doi.org/10.1016/j.jmrt.2019.12.045

electro-rheological fluids [15], electrophoretic displays [19] and corrosion prevention [20]. The first microcapsules-based smart coating was designed in 2001 by White's research group [21]. Microcapsules act as a means of storing and delivering the core material to prevent defect propagation in coatings [22]. Several types of core materials such as dicyclopentadiene (DCPD) [21], epoxy resin [23,24], alkyd resin [25], tung oil [26,27], linseed oil [28–30], organic silanes [30,31], corrosion inhibitors [28,32] and hexamethylene (HMDI) & isophorone (IPDI) based isocyanates have been effectively encapsulated and integrated into polymer matrices to fabricate smart anticorrosion coatings [33–35]. Among all single-component core material, water sensitive isocyanates drew extensive attention due to easy processing and anticorrosion behavior [27,36].

Generally, the capsule walls comprised of carbon-based polymers, such as urea– formaldehyde [20], melamine formaldehyde and polyurethane. Poly-urea formaldehyde (PUF) is extensively used as a microcapsule wall material since it gives good performances of seal, penetration, resistance, flexibility, high strength and impermeability [37,38]. Microcapsules shells were normally fabricated through layer by layer assembly, coacervation, phase separation and interfacial or in situ protocols. In-situ polymerization method is preferred owing to its facile synthesis procedure, low cost, controllable microcapsule size and ease of industrialization [20]. Wu et al. developed PUF shells [39] to stack hexamethylene diisocyanate (HMDI) with increased life span of capsules in organic solvents. Sun et al. [40] used double-layered polyurea shells as HMDI casing for enhanced performance in organic solvents. Sun et al. [41] also studied the effect of double-layered PUF/polyurea compact shell on the shelf life of 4,4′-bis-methylene cyclohexane diisocyanate in water. Urea-formaldehyde (UF) resins have gained importance due to their high reactivity, fast curing, non-flammability, compactness and good thermal properties. UF microcapsule sustains its performance in both organic solvent and water [20]. Anticorrosion behavior of HMDI filled microcapsules were not extensively studied [18,20,42].

Owing to the variety of applications of steel (SS-304) as constructional material in seawater handling such as desalination plants, undersea telecommunications hardware, power plants, subsea pipelines, ships, hulls and submarines, we selected it as principal coating substrate in the present study [43]. Inspite of developing a passive layer of oxide on steel in harsh sea water condition, the excessive chloride ion can induce corrosion thus leading to the degradation of the material and shortening in life time of marine structure.

To achieve better corrosion and wear resistant various mitigation measures are made. Usage of high alloy steel though offers enhanced components durability, but their price and hard machining hamper its application. To overcome these prerequisite, variety of surface treatments like anticorrosive powder coatings, anodizing, nitriding, galvanizing and hard chrome electroplating are used. Hence, there is a dire need to develop better material coatings that are not only environmentally compatible but also can enhance the durability of the components by shielding them from corrosion [44–46].

The aim of this research was to develop and assess the anticorrosion ability of the novel PTF coating on SS-304 substrate. The PTF capsule was synthesized via interfacial polymerization between DETA and isocyanates whereas the crosslinking at the interface of core material (isocyanate) ensures the formation of solid capsule shell. The compact thiourea formaldehyde wall material was selected to circumvent diffusion of the encapsulated HMDI. Moreover, the robust linkage between the host polymer and the microcapsule shell ensures the persistence of the PTF capsule during processing of the matrix [36]. The synthesized PTF microcapsules were dispersed in epoxy (solid content 80 wt%) and subsequently applied on steel substrate SS-304. The effect of salinity, chlorinity, pH, and temperature on the corrosion resistance of SS-304 in harsh corrosive conditions was tested. Finally, the thermally cured PTF coated coupons were subjected to electrochemical impedance spectroscopic studies to evaluate their anticorrosion behavior on SS-304.

**Table 1 – The chemical composition (wt%) of stainless steel (SS-304) substrate.**

| Elements | Cr | Ni | Mn | N | S | C | Si | P | Fe |
|---|---|---|---|---|---|---|---|---|---|
| wt% | 18 | 8.23 | 1.84 | 0.10 | 0.003 | 0.078 | 0.456 | 0.013 | Balance |

**Table 2 – Typical composition of marine water containing various salts and their concentration in g/L.**

| Salts | Concentration (g/L) |
|---|---|
| Sodium chloride | 24.530 |
| Sodium sulfate | 4.0900 |
| Magnesium chloride | 11.100 |
| Calcium chloride | 1.1600 |
| Potassium chloride | 0.6900 |
| Sodium bicarbonate | 0.2000 |
| Potassium bromide | 0.9900 |
| Boric acid | 0.2800 |
| Strontium chloride | 0.0030 |
| Sodium fluoride | 0.0002 |

## 2. Experimental

### 2.1. *Materials and methodology*

Gum Arabic (GA), diethylenetriamine (DETA), 4,4′-diphenylmethane diisocyanate (MDI) prepolymer suprasec 2644, hexamethylene diisocyanate (HMDI), thiourea, ammonium chloride, resorcinol and hydrochloric acid solution (HCl, 0.1 M) were procured from Sigma Aldrich. Salts for the preparation of artificial seawater such as boric acid, calcium chloride, magnesium chloride, potassium chloride, sodium hydroxide, sodium chloride, sodium sulfate, sodium bicarbonate, strontium chloride and sodium fluoride were purchased from Riedel-De-Haen. The blend of bisphenol A (resin) and polyamide (hardener) were used as an epoxy coating. All the chemicals in this study were used as purchased with no additional purification. The chemical composition of the investigated steel SS 304 is shown in Table 1 [45].

The electrolyte used for electrochemical studies in the present study was artificial seawater. It was prepared according to ASTM D1141 standard method by using exact concentrations of various salts such as chlorides, sulfates, carbonates and bicarbonates [24,47]. About 41.953 g of salts were dissolved in distilled water to prepare 1 L of seawater and pH

of the solution was adjusted to 8.3 by adding few drops of 0.1 M NaOH and 0.1 M HCl aqueous solutions. Table 2 shows the typical composition of marine water containing various salts and their concentration in g/L [48].

SS-304 substrate sheets were initially abraded with 600, 800 and 1200 grit emery paper followed by casting into coupons of $1 \times 1\,cm^2$. These coupons were then conditioned by immersion in NaOH solution of pH~10 for two minutes to make it pregnable and to activate its terminal group for proper adhesion. Finally, the coupons were washed three times with freshly distilled water and rinsed with acetone.

### 2.2. Synthesis

The encapsulation of HMDI leading to the synthesis of poly-thiourea formaldehyde dual-shelled microcapsule was accomplished by the complimentary polymerization techniques namely interfacial and in situ polymerization. Firstly, the microcapsules were synthesized using interfacial polymerization in an oil-in-water blend. At the outset, gum Arabic (2.5 wt%) was dissolved in 30 mL of deionized water and the surfactant solution was heated at 30 °C to obtain a homogenous aqueous phase. Afterwards, the uniform oil phase containing 4.5 g of HMDI and 0.5 g of MDI was emulsified in the surfactant aqueous solution (A) under certain agitation speed. Once the system was stabilized at 30 °C for 45 min, 18 g of DETA solution (30 wt%) was added to instigate the interfacial polymerization (B). Meanwhile, temperature of the suspension was elevated to 65 °C and kept for 30 min. The slurry of thiourea microcapsule was subsequently washed with deionized water for 3–4 times [27].

In another beaker (C) containing 60 mL of deionized water, 2 g of thiourea was dissolved in 0.5 g of both ammonium chloride and resorcinol solution. To ensure thorough mixing, an agitation rate of 200 rpm was maintained and pH of the solution was tuned from neutral to approximate pH 3 using HCl and NaOH aqueous solutions. The previously synthesized capsules were poured into the solution (C) after stabilization at 55 °C. After a further reaction for 20 min, formaldehyde solution (37 wt%/4.5 mL) was added in suspension (D) to develop a topcoat of formaldehyde on thiourea microcapsules. The capsules suspension was washed with deionized water three times prior to air drying for 12 h. The complete schematic of the synthesis of multilayered poly-thiourea formaldehyde microcapsules is explicitly illustrated in Fig. 1.

Poly-thiourea formaldehyde coatings were made by the blend of PTF capsules in acetone under stirring at 200 rpm for 5 min at RT. Bisphenol-A (epoxy resin) and xylene were introduced to the mixture, followed by the addition of polyamide (curing agent). The same solution was kept for 15 min after continuous stirring at 200 rpm. The coating layers were applied onto the SS-304 steel substrates via a drawdown bar with a wet thickness of about 500 μm. The wet films were placed in a dust free chamber for 24 h, followed by thermal curing at 60 °C for 1 h. All cured films were kept at ambient conditions for 3 days before testing. Different weight% of PTF microcapsules were incorporated into epoxy to formulate coating system as shown in Table 3.

### 2.3. Characterization

Fourier transform infrared study of poly-thiourea formaldehyde microcapsules was performed for functional group identification employing the FTIR spectrometer (Perkin Elmer Spectrum One (Ver. B)) at room temperature. Thermal behavior of the synthesized capsules was recorded using Toledo Perkin Model Q 500, at the heating rate of 10 °C/min in an argon atmosphere. To examine water resistance, PTF capsules were immersed in open air and water solution with different pH values (pH 1 and pH 11) for a certain duration to observe the effect on relative core fraction. TGA was performed to ascertain the thermal stability and residual core fraction of PTF capsules. Acetone immersion method was used to measure the core content of HMDI in capsules.

$$C_{shell} + C_{core} = C_{microcapsules} \quad (1)$$

Encapsulation efficacy was calculated from the mass of the resultant PTF capsules ($W_m$) over the preliminary weight of all the reactants (HMDI and pre-TUF).

$$\text{Microencapsulation efficiency} = [W_m / (W_{HMDI} + W_{pre\text{-}TUF})] \times 100\% \quad (2)$$

The surface morphology and particle size characterization of the PTF coated substrates was carried out using a JEOL 6700F field emission microscope. Finally, the electrochemical studies were carried out by potentiodynamic polarization and electrochemical impedance spectroscopy (EIS) using Gamry instrument reference 3000 potentiostat/galvanostat ZRA (Zero resistance ammeter). A three-electrode set-up comprising of a saturated calomel (reference electrode), graphite (counter electrode) and steel coupon with an exposed area of $1 \times 1\,cm^2$ (working electrode) was used. To achieve stabilization, all the test samples were soaked in an artificial seawater, one day prior to the electrochemical test. Spectra were obtained in the frequency range from $10^6$ to $10^{-2}$ with an AC amplitude of 10 mV. Data fitting was done using Echem Analyst software version 6.33.

## 3. Results and discussion

The PTF smart coatings were synthesized through an established in situ polymerization reaction as reported elsewhere [49]. The pictorial representation of the encapsulation of HMDI by poly-thiourea microcapsules followed by formaldehyde topcoat in an oil-and-water emulsion system is shown schematically in Fig. 1.

### 3.1. FT-IR studies

The FT-IR spectra of the core material, pure HMDI, suprasec 2644 (MDI), fresh and processed PTF microcapsules are shown in Fig. 2. The characteristic vibration bands of all the components of poly-thiourea microcapsules were in good agreement with the literature values [41]. The processed microcapsules were prepared by preserving fresh shell material for

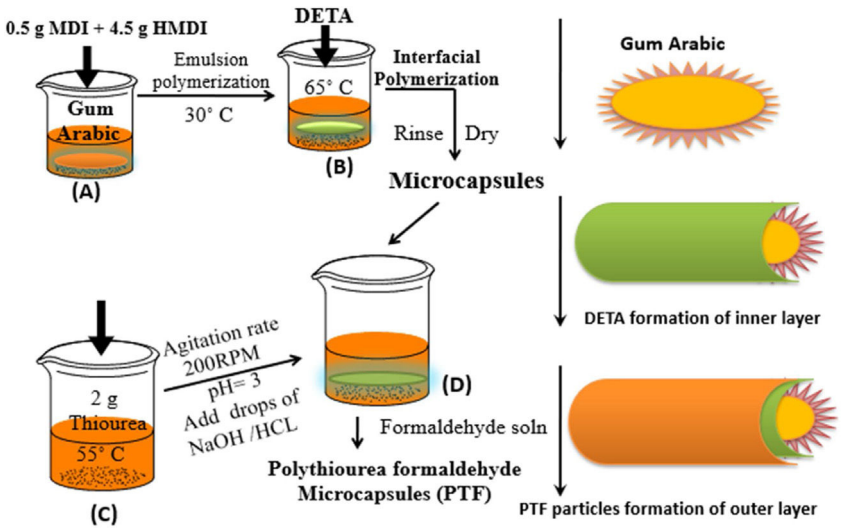


**Fig. 1 – Scheme for the synthesis of poly-thiourea formaldehyde-based coatings.**

**Table 3 – Composition of poly(thiourea) formaldehyde coatings.**

| Sr. no | Microcapsules (wt%) | Epoxy (g) | Hardener (g) | Filler (g) | Solvent (mL) |
|---|---|---|---|---|---|
| 1 | 1 wt%-PTF | 5 | 6.7 | 0.2 | 7 |
| 2 | 5 wt%-PTF | 5 | 6.7 | 0.2 | 7 |
| 3 | 10 wt%-PTF | 5 | 6.7 | 0.2 | 7 |

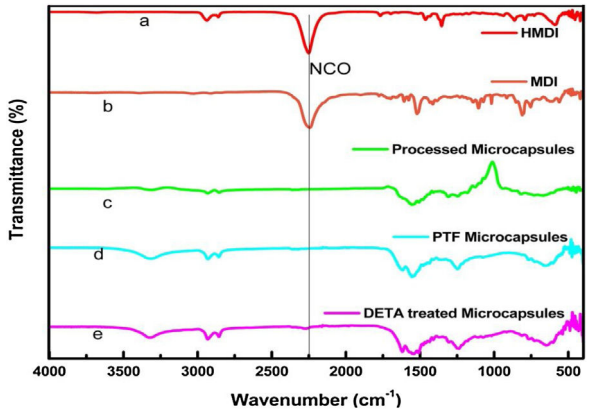


**Fig. 2 – The IR spectra of a) HMDI b) MDI c) processed microcapsules d) PTF microcapsules e) DETA treated microcapsules.**

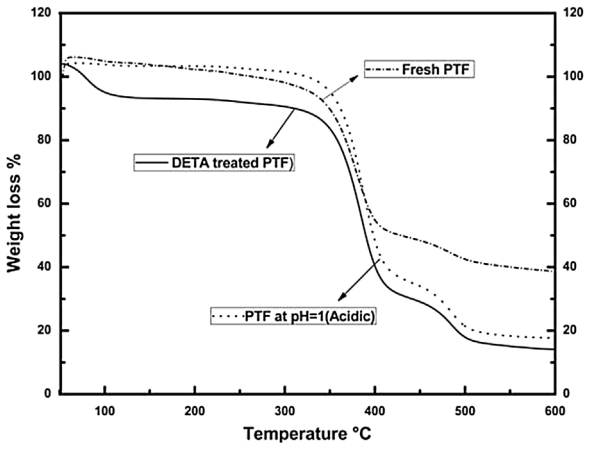


**Fig. 3 – Thermogravimetric curves of the fresh and processed poly-thiourea formaldehyde microcapsules.**

5 days in DETA solution and in an aqueous solution of pH 1 respectively. The IR spectrum of HMDI and core material was nearly alike indicating the effective HMDI encapsulation. However, the subtle phenyl group stretches at 1642 $cm^{-1}$ and 1543 $cm^{-1}$ were still detected ensuring the connectivity of the suprasec 2644 within the capsule by diffused DETA and water molecules. Conversely, the –NCO signal at 2271 $cm^{-1}$ was still observed in the spectrum of shell. During the reaction process, the high crosslinking density restricts the continuous depletion of residual –NCO groups by diffusion-in water. The presence of NCO band within the spectrum of fresh shell is primarily due to the compact shell wall, which confirms the absence of the unreacted NCO groups. On the other hand, the vanishing of this NCO band from 2271 $cm^{-1}$ after shell processing validates the reactivity of NCO group thus ensuring the effective inclusive incorporation of HMDI.

### 3.2. *Water resistance and thermal stability of anticorrosive PTF microcapsules*

The weight loss curves of fresh and processed PTF microcapsules as a function of temperature were recorded using thermogravimetry as illustrated in Fig. 3. Thermal properties of PTF microcapsules at various synthesis stages were also investigated. PTF microcapsules were soaked in DETA solution

meanwhile their tolerance to a highly acidic solution of pH 1 and subsequent temperature stability was also checked. The thermograms of treated microcapsules were finally recorded after completely drying at RT. Fresh PTF microcapsules started to lose weight below 100 °C due to the presence of free formaldehyde. However, the first major weight loss is seen between 176 °C to 184 °C owing to slow degradation till 394 °C. Second major weight loss occurs between 416 °C to 425 °C attributed to the disintegration of the core material (HMDI) with complete decomposition around 600 °C. We observed a steady weight loss at 169 °C beckoning toward the HMDI weight loss because of small shell thickness and larger surface area in line with the literature [41]. It is reported that pure HMDI loses weight at 169 °C and starts evaporating only because of small shell thickness and larger surface area [41]. Ultimately, we found out that fresh PTF microcapsules are more thermally stable compared with their processed capsules as indicated by high char yield of 39 wt% whereas char yield of 17 wt% and 18 wt% was found for acid soaked and DETA treated PTF microcapsules.

Water resistance of these anticorrosive smart coatings was envisaged by immersing fresh capsules in acidic and alkaline solutions respectively. The relative core fraction decreased steadily with increasing immersion time in both acidic and alkaline solutions. The relative core fraction was 83% (Eq. (1)) in alkaline (pH 11) and 79% in acidic media (pH 1) respectively. Diffusion of $H_2O$ molecule s in microcapsules under longer immersion time consumes more core material (HMDI). Conversely, the exceptional stability in buffered solutions protects encapsulated PTF microcapsules.

The pot life of synthesized poly thiourea formaldehyde (PTF) microcapsules was assessed by exposure to air and immersion in water at various temperatures. It is revealed that higher temperature accelerates the diffusion of $H_2O$ molecules and increases shell porosity leading to low durability of PTF microcapsules in warm water. The core content of PTF capsules was measured by acetone immersion technique, the value was around 82% (Eq. (1)). This high core filling leads to higher encapsulation efficiencies of PTF microcapsules. The encapsulation yield was $63 \pm 2.1\%$ (Eq. (2)), lesser than 100%, which was due to polymerization of pre-TUF to the PTF units during the formation of the casing. As assessed by weight loss measurements, in damp air the relative core fraction reached 94.2% residue after 21 days. Additionally, a similar decreasing trend was observed in relative core fraction of PTF capsules immersed in water at room temperature with 92% residue left after 21 days. The penetration of water molecules into the capsules led to a decrease in residual content in comparison to open air. Unique PTF shell material contributed to the notable water resistance yet, the core material was entirely depleted after 14 days in 30 °C and 7 days in 40 °C.

### 3.3. *Factors affecting the particle size, morphology and corrosion onset*

The shell compactness and size of the PTF capsules were monitored with a scanning electron microscopy as shown in Fig. 4a. For calculating the mean diameter, 200 individual capsules were measured. The average particle size of poly-thiourea microcapsules greatly depends on the rate of agitation. Higher

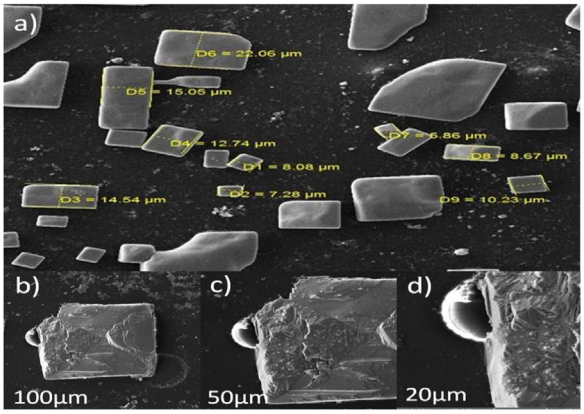


**Fig. 4 – SEM micrographs of PTF microcapsule demonstrating the a) particle size distribution and b), c) and d) morphology of HMDI containing PTF microcapsule at varied magnification (100 µm → 20 µm).**

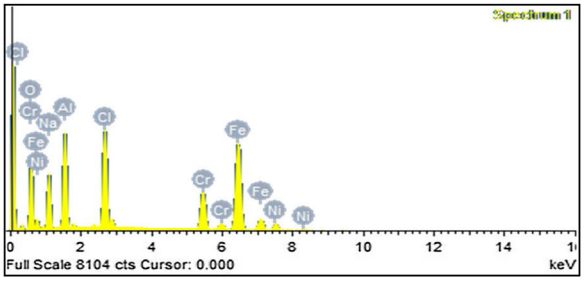


**Fig. 5 – EDX spectrum of bare SS-304 after exposure to artificial sea water.**

the rate of agitation smaller is the particle size and vice versa. In the present study, SEM results show that the microcapsules have coarse outer layer, random particle size distribution with uniform morphology. Particle size was found in the range of 1.08 µm–22.06 µm. These microcapsules were filled with catalyst-free healing agent HMDI, which was protected by a shell and is not in contact with the polymer matrix directly until subjected to a rupture propagating cracks in the matrix. SEM images of coatings after electrochemical studies depicted the signature of salt deposition due to corrosion with slight rupturing of microcapsules. Once the corrosion has occurred, the loaded core material (HMDI) started to ooze out into the cracks via capillary action as shown in Fig. 4.

SEM micrographs of SS-304 coated substrate revealed the surface damage in the form of small corrosion pits. Reddish brown corrosion deposits were also observed on the bare metal surface. EDX further evidenced the deposition of various salts namely hematite metal oxide ($Fe_2O_3$) rusting the metal surface along with deposition of sodium and chloride ions. Compositional analysis of metal surface shows an increase in overall wt% of Fe as investigated by EDX. This means that SS-304 is slowly degraded due to enhanced exposure to an aggressive electrolyte. Fig. 5 shows the EDX spectrum of bare SS-304 after exposure to artificial seawater for seven days. SEM micrographs revealing corrosion signature at gradually decreasing magnification as depicted in the Fig. 6. While Table 4 gives the

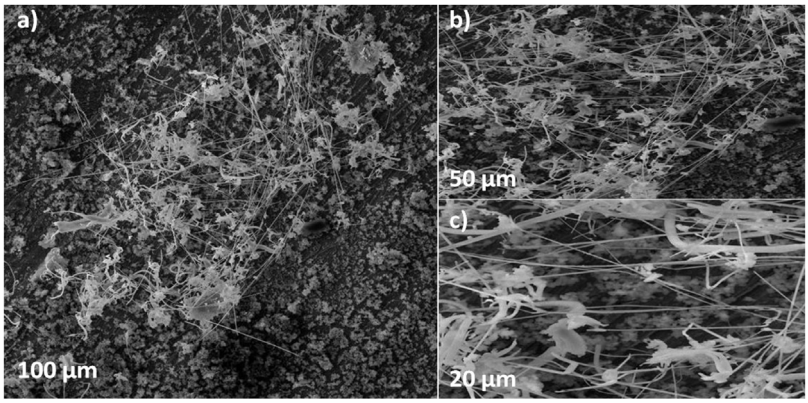


**Fig. 6 – SEM micrographs showing corrosion effects on bare steel immersed in seawater for 1-week a) 100-µm b) 50-µm c) 20-µm.**

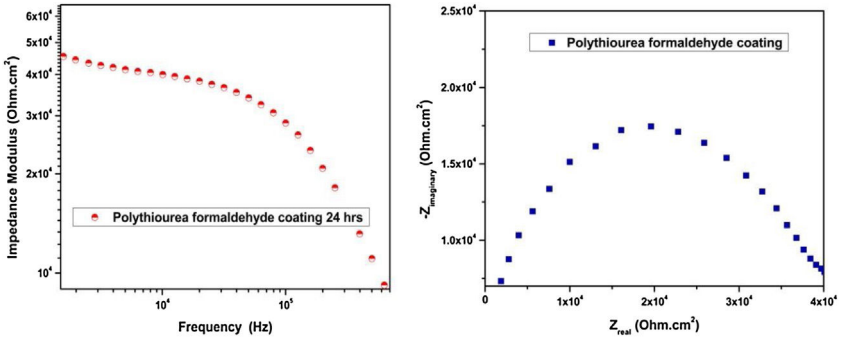


**Fig. 7 – The impedance modulus vs frequency curve on the left and Nyquist plot of PTF coated SS-304 on right.**

**Table 4 – Elemental composition of SS-304 after prolonged exposure to seawater.**

| Element | Weight% | Atomic% |
|---|---|---|
| O | 17.5 | 34.1 |
| Na | 11.3 | 15.2 |
| Al | 11.5 | 13.2 |
| Cl | 12.1 | 10.6 |
| Cr | 9.70 | 5.80 |
| Fe | 34.1 | 19.0 |
| Ni | 3.62 | 1.92 |

elemental composition of the same substrate after prolonged exposure to seawater.

### 3.4. *Electrochemical corrosion studies*

PTF coatings were monitored by EIS and potentiodynamic polarization measurements by means of Gamry Reference 3000 potentiostat/galvanostat. The impedance and potentiodynamic measurements were also recorded with reference to open circuit potentials (OCP). The electrochemical set up was kept for 20 min prior to the measurements in order to get stable OCP. Fig. 7 shows the impedance modulus versus frequency plot together with nyquist plot for PTF coated SS-304 in artificial seawater. $R_{soln}$, $R_{po}$, $E_{corr}$, $I_{corr}$, and corrosion rate were obtained by using E-Chem analyst software. Nyquist results illustrate the improvement in behavior of PTF coating compared to bare metal under similar conditions. Table 5 sorts out various impedance and polarization parameters calculated after electrochemical testing and subsequent Reap2cpe model fitting of bare ($1 \times 1\,cm^{-2}$) and PTF coated (10 wt%) steel coupons. All the measurements were performed thrice to guarantee the reproducibility of outcome.

Quantification of corrosion protection efficiency of PTF coatings was done using potentiodynamic polarization with artificial seawater as electrolyte. $E_{corr}$ value obtained for PTF coated SS-304 (−63.2 mV) was more positive than that for the bare steel (−125 mV) indicating the superior corrosion protection. The positive shift in $E_{corr}$ values demonstrates the improved protection efficiency of PTF coating on SS-304. Moreover, the corrosion shielding efficiency was significantly enhanced by increasing the microcapsule loading (i.e

**Table 5 – Electrochemical corrosion measurements of bare and PTF coated SS-304.**

| System | $R_{soln}$ (Ω) | $R_{po}$ (Ω) | $I_{corr}$ (µA) | $E_{corr}$ (mV) | $R_{corr}$ (mpy) |
|---|---|---|---|---|---|
| Bare SS-304 | 4.28 | 1.69 | −74.3 | −125 | 2.1 |
| PTF coated SS-304 (10 wt%) | 90.5 | 30.9 | −0.08 | −63.2 | 1.2 |

1–10 wt%). The calculated corrosion current ($I_{corr}$) for PTF coated steel electrode was lower than the uncoated counterpart and corresponds to a corrosion rate ($R_{corr}$) of about 1.2 mpy. Significantly higher polarization resistance ($R_{po}$) was observed for the PTF coated substrate in artificial seawater. Consequently, based on the results of electrochemical measurements, PTF coated strips offer better corrosion resistance than uncoated coupons.

## 4. Conclusion

The coalescence of interfacial and in-situ polymerization methods used for incorporation of HMDI in poly-thiourea formaldehyde (PTF) shell was studied. The characteristic -NCO peak (2200 $cm^{-1}$) in FT-IR endorsed the effective encapsulation of core material (HMDI) into the capsule. The influence of experimental parameters on the encapsulation process was systematically investigated. The results illustrate that the preparation of PTFs is highly dependent on the synthesis conditions. The agitation rate controls the diameter of the microcapsules; the higher core loading leads to higher encapsulation efficiencies of capsules, whereas the solution pH value in the range of 3–7 is found to be optimum for the synthesis of PTF capsules. From TGA results, freshly synthesized PTF capsules were observed to be more stable compared with their processed capsules. The coarse morphology of microcapsule shell revealed via SEM has offered a good anchoring between capsule and epoxy matrix. Electrochemical measurements disclose that PTF coating displayed quite good corrosion protection ability to steel substrate as is evident from lower $R_{corr}$ value of about 1.2 mpy compared to bare SS-304. Further measurements including TEM studies are underway to understand the potential self-healing ability of synthesized PTF microcapsules.

## Declaration of Competing Interest

The authors declare that they have no known competing financial interests or personal relationships that could have appeared to influence the work reported in this paper.

## Acknowledgement

N.Z. Ali gratefully acknowledges the funding received from the Directorate of Research & Academic Coordination (RAC) National Centre for Physics Islamabad, Pakistan.

REFERENCES

[1] Fedel M, Deflorian F, Rossi S, Kamarchik P. Progress in organic coatings study of the effect of mechanically treated $CeO_2$ and $SiO_2$ pigments on the corrosion protection of painted galvanized steel. Prog Org Coat 2012;74(1):36–42.
[2] Abdullayev E, Price R, Shchukin D, Lvov Y. Halloysite tubes as nanocontainers for anticorrosion coating with benzotriazole. ACS Appl Mater Interfaces 2009:1437–43.
[3] Alibakhshi E, Ghasemi E, Mahdavian M, Ramezanzadeh B. A comparative study on corrosion inhibitive effect of nitrate and phosphate intercalated Zn–Al-layered double hydroxides (LDHs) nanocontainers incorporated into a hybrid silane layer and their effect on cathodic delamination of epoxy topcoat. Eval Program Plann 2016;115:159–74.
[4] Zhu DY, Rong MZ, Zhang MQ. Self-healing polymeric materials based on microencapsulated healing agents: from design to preparation. Prog Polym Sci 2015;49–50:175–220.
[5] Alibakhshi E, Ghasemi E, Mahdavian M. Progress in organic coatings optimization of potassium zinc phosphate anticorrosion pigment by Taguchi experimental design. Prog Org Coat 2013;76(1):224–30.
[6] Alibakhshi E, Ghasemi E, Mahdavian M, Ramezanzadeh B. A comparative study on corrosion inhibitive effect of nitrate and phosphate intercalated Zn–Al-layered double hydroxides (LDHs) nanocontainers incorporated into a hybrid silane layer and their effect on cathodic delamination of epoxy topcoat. Eval Program Plann 2017;115:159–74.
[7] Alibakhshi E, Akbarian M, Ramezanzadeh M, Ramezanzadeh B, Mahdavian M. Progress in organic coatings evaluation of the corrosion protection performance of mild steel coated with hybrid sol–gel silane coating in 3.5 wt % NaCl solution. Prog Org Coat 2018;123(June):190–200.
[8] Ferreira MGS, Duarte RG, Montemor MF, Simões AMP. Silanes and rare earth salts as chromate replacers for pre-treatments on galvanised steel. Electrochim Acta 2004;49(17–18):2927–35.
[9] Ramezanzadeh B, Akbarian M, Ramezanzadeh M, Mahdavian M, Alibakhshi E, Kardar P. Corrosion protection of steel with zinc phosphate conversion coating and post-treatment by hybrid organic–inorganic sol–gel based silane film. J Electrochem Soc 2017;164(6): C224–30.
[10] Alibakhshi E, Ghasemi E, Mahdavian M. The influence of surface modification of lithium zinc phosphate pigment on corrosion inhibition of mild steel and adhesion strength of epoxy coating. J Sol Gel Sci Technol 2014:359–68.
[11] Plawecka M, Snihirova D, Martins B, Szczepanowicz K, Warszynski P, Montemor MF. Self healing ability of inhibitor-containing nanocapsules loaded in epoxy coatings applied on aluminium 5083 and galvanneal substrates. Electrochim Acta 2014;140:282–93.
[12] Alibakhshi E, Akbarian M, Ramezanzadeh M, Ramezanzadeh B, Mahdavian M. Progress in organic coatings evaluation of the corrosion protection performance of mild steel coated with hybrid sol–gel silane coating in 3.5 wt% NaCl solution. Prog Org Coat 2018;123(December):190–200.
[13] Patravale VB, Mandawgade SD. Novel cosmetic delivery systems: an application update. Int J Cosmet Sci 2008;30(1):19–33.
[14] Nejman A. Methods of PCM microcapsules application and the thermal properties of modified knitted fabric. Thermochim Acta 2014;589:158–63.
[15] Patravale VB, Mandawgade SD. Novel cosmetic delivery systems: an application update. Int J Cosmet Sci 2008:19–33.
[16] Kulčar R, Friškovec M, Hauptman N, Vesel A, Gunde MK. Colorimetric properties of reversible thermochromic printing inks. Dyes Pigm 2010;86(3):271–7.
[17] Kumar A, Stephenson LD, Murray JN. Self-healing coatings for steel. Prog Org Coat 2006;55(3):244–53.
[18] Damasceno S, Pereira GR. Eddy current and inspection of coatings for storage. Integr Med Res 2018;(x x):6–10.
[19] Chuanjie F, Juntao T, Xiaodong Z. Effects of process parameters on the physical properties of poly(urea-formaldehyde) microcapsules prepared by a one-step method. Iran Polym J (English Ed) 2013;22(9):665–75.
[20] Katoueizadeh E, Zebarjad SM, Janghorban K. Investigating the effect of synthesis conditions on the formation of urea-formaldehyde microcapsules. Integr Med Res 2018;(x x):1–12.

[21] Yang J, et al. Microencapsulation of isocyanates for self-healing polymers microencapsulation of isocyanates for self-healing polymers. Macromolecules 2008;41(November):9650–5.
[22] Asadi AK, Ebrahimi M, Mohseni M. Microencapsulation of a sunlight curable silicon based resin in the presence of polyvinylpyrrolidone. Pigment Resin Technol 2017;47(3):272–8.
[23] Liu X, Zhang H, Wang J, Wang Z, Wang S. Preparation of epoxy microcapsule based self-healing coatings and their behavior. Surf Coat Technol 2012;206(23):4976–80.
[24] Liao LP, Zhang W, Zhao Y. Preparation and healing property evaluation of self-repairing polymer coating. Surface Engineering 2014;30(2):138–41, http://dx.doi.org/10.1179/1743294413Y.0000000216.
[25] Khorasani SN, Ataei S, Neisiany RE. Microencapsulation of a coconut oil-based alkyd resin into poly(melamine–urea–formaldehyde) as shell for self-healing purposes. Prog Org Coat 2017;111(February):99–106.
[26] Samadzadeh M, Boura SH, Peikari M, Ashrafi A, Kasiriha M. Tung oil: an autonomous repairing agent for self-healing epoxy coatings. Prog Org Coat 2011;70(4):383–7.
[27] Li H, Cui Y, Li Z, Zhu Y, Wang H. Fabrication of microcapsules containing dual-functional tung oil and properties suitable for self-healing and self-lubricating coatings. Prog Org Coat 2018;115(November):164–71.
[28] Suryanarayana C, Rao KC, Kumar D. Preparation and characterization of microcapsules containing linseed oil and its use in self-healing coatings. Prog Org Coat 2008;63(1):72–8.
[29] Behzadnasab M, Mirabedini SM, Esfandeh M, Farnood RR. Evaluation of corrosion performance of a self-healing epoxy-based coating containing linseed oil-filled microcapsules via electrochemical impedance spectroscopy. Prog Org Coat 2017;105:212–24.
[30] Thanawala K, Mutneja N, Khanna AS, Raman RKS. Development of self-healing coatings based on linseed oil as autonomous repairing agent for corrosion resistance. Materials 2014:7324–38.
[31] Huang M, Zhang H, Yang J. Synthesis of organic silane microcapsules for self-healing corrosion resistant polymer coatings. Corros Sci 2012;65:561–6.
[32] Mehta NK, Bogere MN. Environmental studies of smart/self-healing coating system for steel. Prog Org Coat 2009;64:419–28.
[33] Wang W, Xu L, Li X, Yang Y, An E. Self-healing properties of protective coatings containing isophorone diisocyanate microcapsules on carbon steel surfaces. Corros Sci 2014;80:528–35.
[34] Haghayegh M, Mirabedini SM, Yeganeh H. Microcapsules containing multi-functional reactive isocyanate-terminated polyurethane prepolymer as a healing agent. Part 1: synthesis and optimization of reaction conditions. J Mater Sci 2016;51(6):3056–68.
[35] Sun D, An J, Wu G, Yang J. Double-layered reactive microcapsules with excellent thermal and non-polar solvent resistance for self-healing coatings. J Mater Chem A 2015;3(8):4435–44.
[36] Sun D, Bing Y, Chen K, Yang J. Chemically and thermally stable isocyanate microcapsules having good self-healing and self-lubricating performances. Chem Eng J 2018;346(December):289–97.
[37] Çömlekçi GK, Ulutan S. Encapsulation of linseed oil and linseed oil based alkyd resin by urea formaldehyde shell for self-healing systems. Prog Org Coat 2018;121(April):190–200.
[38] Qin R, Xu G, Guo L, Jiang Y, Ding R. Preparation and characterization of a novel poly(urea-formaldehyde) microcapsules with similar reflectance spectrum to leaves in the UV–vis-NIR region of 300–2500 nm. Mater Chem Phys 2012;136(2–3):737–43.
[39] Wu G, An J, Tang X, Xiang Y, Yang J. A versatile approach towards multifunctional robust microcapsules with tunable, restorable, and solvent-proof superhydrophobicity for self-healing and self-cleaning coatings. Mater Sci 2014:6751–61.
[40] Sun D, An J, Wu G, Yang J. Excellent thermal and non-polar solvent resistance. J Mater Chem A Mater Energy Sustain 2015;00:1–10.
[41] Sun D, Zhang H, Tang X, Yang J. AC SC. Polymer (Guildf) 2016.
[42] Khodair ZT, Khadom AA, Jasim HA. Corrosion protection of mild steel in different aqueous media via epoxy/nanomaterial coating: preparation, characterization and mathematical views. Integr Med Res 2018;(x x):1–12.
[43] Ul-hamid A, Saricimen H, Quddus A, Mohammed AI. Corrosion study of SS304 and SS316 alloys in atmospheric, underground and seawater splash zone in the Arabian Gulf. Corros Eng Sci Technol 2017;52(2):134–40.
[44] Malik AU, Ahmad S, Andijani I. Corrosion behavior of steels in gulf sea water environment. Desalination 1999;123(February):205–13.
[45] Atashin S, Toloei AS, Pakshir M. Simultaneous investigation of marine factors effect on corrosion rate of ss 304 in turbulent condition. J Mater Eng Perform 2013;22(7):2038–47.
[46] Mollica A, Trevis A, Traverso E, Ventura G, De Carolis G, Dellepiane R. Crevice corrosion resistance of stainless steels in natural seawater in the temperature range of 25 to 40 C. Corrosion 1988;44(4):194–8.
[47] Hoseinieh SM, Shahrabi T. Influence of ionic species on scaling and corrosion performance of AISI 316L rotating disk electrodes in artificial seawater. Desalination 2017;409:32–46.
[48] Cao F, Zhao C, You J, Hu J, Zheng D. The inhibitive effect of artificial seawater on magnesium corrosion. Adv Eng Mater 2019:1–14, 1900363.
[49] Li H, Cui Y, Li Z, Zhu Y, Wang H. Fabrication of microcapsules containing dual-functional tung oil and properties suitable for self-healing and self-lubricating coatings. Prog Org Coat 2018;115(July):164–71.